

INDUSTRIAL CROPS AND PRODUCTS

AN INTERNATIONAL JOURNAL



Fabrication of chitosan-encapsulated microcapsules containing wood wax oil for antibacterial self-healing wood coatings

EI检索

SCI升级版 农林科学1区

SCI基础版 农林科学1区

IF 6.2

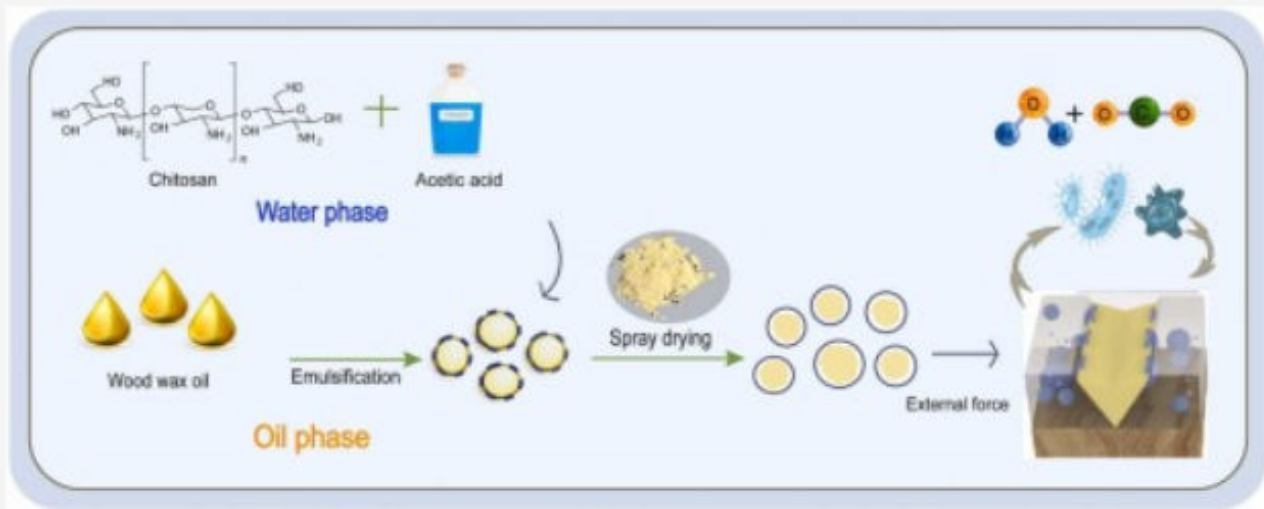
Industrial Crops and Products, 15 December 2024

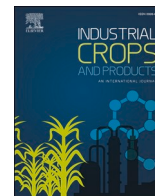
Yijuan Chang, Zhihui Wu, Enwen Liu

Abstract ▾

Graphical Abstract ▲

Export ▾





Fabrication of chitosan-encapsulated microcapsules containing wood wax oil for antibacterial self-healing wood coatings

Yijuan Chang^a, Zhihui Wu^{a,b,*}, Enwen Liu^a

^a College of Furnishings and Industrial Design, Nanjing Forestry University, Nanjing 210037, China

^b Co-Innovation Center of Efficient Processing and Utilization of Forest Resources, Nanjing Forestry University, Nanjing 210037, China

ARTICLE INFO

Keywords:

Wood wax oil
Chitosan
Microcapsule
Self-healing
Antibacterial
Coating

ABSTRACT

Wood multifunctional smart coating is a new functional coating that combines smart material technology with traditional wood. In this study, wood wax oil based on thistle oil and flaxseed oil was used as the core material, and chitosan was used as the wall material to prepare self-repairing antibacterial microcapsules. The optimal preparation conditions were found to be an oil-water ratio (OWR) of 2:1, a core-to-wall ratio of 3:1, using OP-10 as the emulsifier at a concentration of 10.0 %, and a crosslinker concentration of 0.18 g/mL. The encapsulation efficiency of microcapsules was 73.7 % by spray drying, and the thermal stability was improved. The chitosan microcapsules exhibit the characteristics of water sensitivity and acid selective response, with rapid release at pH 7.0. Blending microcapsules at concentrations of 2.0 %, 5.0 %, and 8.0 % with UV topcoat and applying them to walnut plywood resulted in a multifunctional wood coating. Artificially simulated daily scratch damage was effectively repaired within 7 d. Furthermore, the 10.0 % microcapsules demonstrated antibacterial properties against *Escherichia coli* (*E. coli*) and *Escherichia coli* (*E. coli*), with an antibacterial *E. coli* and *S. aureus* rate of up to 75.82 % and 42.96 %. The IC₅₀ of the wood coatings against *E. coli* was 5.667, while against *S. aureus* it was 15.45. The minimum inhibitory concentration (MIC) of the microcapsules against both *E. coli* and *S. aureus* was 10.0 %. The coating film containing 2.0 % microcapsules demonstrated superior overall performance. This research established a foundation for the development of self-healing antibacterial coatings for wood and addressed the gap in dual-functional self-healing antibacterial paint films for wood.

1. Introduction

The coating formed by wood coatings on wood can protect and beautify the surface of the wood, seal the pores of the wood, and improve the stability of the wood (De Meijer, 2001). It can also provide special functions such as antibacterial (Zou et al., 2023; Zou et al., 2024), waterproofing (Janesch et al., 2020), fire protection for the wood (Wang et al., 2019) and composite functional coating (Zhu et al., 2024). Ultraviolet (UV) coating has become a commonly utilized and significant technique for adjusting the surface properties of wood (Xia et al., 2024). This technique is favored for its numerous advantages, including rapid drying, the formation of a robust paint film, and enhanced resistance to aging and wear. (Liu et al., 2020; Rawat et al., 2019). However, UV coatings are susceptible to damage from environmental factors during use, which can adversely affect their structure and various performance characteristics (Wu et al., 2020). Additionally, these coatings exhibit low hardness, poor elasticity, and a tendency to yellow over time

(Chang and Chou, 2000). They are prone to damage due to the deterioration of the wooden substrate, with factors such as wet expansion and dry shrinkage contributing to the formation of microcracks. Extending the service life of these coatings to enhance the protection of the wood substrate is a significant area of research in the field of coatings. Therefore, adjusting the characteristics of wood surface coating and suppressing its cracking defects has important theoretical exploration and practical significance.

Microencapsulation is a technology for encapsulating active substances (Gouin, 2004). It is a process of encapsulating a small amount of active chemicals in a thin layer of polymer (Zhang et al., 2023). This technology reveals huge potential for enhancing product performance (Bakry et al., 2016). It regulates the release of volatile ingredients, prevents their oxidation, and enhances their efficacy and durability (Nesterenko et al., 2014). The mechanism of substance release is determined by the form of the shell material and the density, permeability and biological properties of the shell material (Abbaspourrad

* Corresponding author at: College of Furnishings and Industrial Design, Nanjing Forestry University, Nanjing 210037, China.

E-mail addresses: changyijuan@njfu.edu.cn (Y. Chang), wzh550@sina.com (Z. Wu), lew@njfu.edu.cn (E. Liu).

<https://doi.org/10.1016/j.indcrop.2024.119438>

Received 16 June 2024; Received in revised form 26 July 2024; Accepted 14 August 2024

Available online 28 August 2024

0926-6690/© 2024 Elsevier B.V. All rights reserved, including those for text and data mining, AI training, and similar technologies.

et al., 2013). In previous study, self-healing microcapsule have been widely studied as external repair methods. Most wall materials used are melamine resin and urea-formaldehyde resin, but no matter how they are modified, the release of formaldehyde cannot be avoided (Fei et al., 2015). Chitosan has unlimited potential as a microcapsule wall material (Meng et al., 2023). The main preparation method of chitosan-based microcapsules is ion crosslinking, which usually uses sodium tripolyphosphate (STPP) and chitosan for ion electrostatic adsorption to induce gelation (Yousefi et al., 2019; Mwangi et al., 2016).

In recent years, the application of chitosan-based microcapsules in biomedical and food science has become increasingly widespread, demonstrating the enormous practical potential of chitosan microcapsules (Budinić et al., 2021), especially chitosan-based antibacterial microcapsules (Ding and Yan, 2024; Lai et al., 2021). Due to the progression of the COVID-19 pandemic, the development of various antimicrobial materials, including antimicrobial coatings and antibacterial fabric (Koçak and Yılmaz, 2022; Yılmaz, 2023), has become a priority in the pursuit of sustainable development. (Kumar et al., 2020; Yılmaz and Bahtiyari, 2020). The focus is on the antibacterial effects of natural antibacterial substances on the negative carrier (Yılmaz, 2020). The pH-responsive cellulose-based microcapsules prepared by Wu Min et al. at pH 4.0, the membrane was effective against *Escherichia coli* and *Listeria monocytogenes*. The inhibition rate of bacteria reached 99.0 % (Wu et al., 2024). Research on self-healing coatings induced by the implantation of microcapsules has become increasingly advanced (Rawat et al., 2019; Samadzadeh et al., 2010), but studies that integrate these two aspects are scarce (Deng et al., 2023). To date, there have been no reports in the literature on chitosan encapsulated wood wax oil microcapsules. Wood wax oil offers numerous advantages, including high permeability, moisture resistance, anti-corrosion properties, insect resistance, flame retardancy, UV resistance, and the absence of harmful odors. (Janesch et al., 2020). As demonstrated in our previous research, wood wax oils based on thistle oil and linseed oil exhibited substantial antioxidant properties (Chang and Wu, 2024). Utilizing wood wax oil as a core repair agent addresses the need for sustainable, wear-resistant coatings. By incorporating self-healing antibacterial microcapsules into wood coating systems, the toughness and mechanical properties of the coatings are enhanced through microstructural adjustments. This integration also improves the coatings' antibacterial performance and their resistance to environmental factors.

In this study, pH-responsive self-healing antibacterial microcapsules were prepared by coating wood wax oil microcapsules with chitosan to promote the antibacterial and self-healing of wood coatings. The healing agent (wood wax oil) is encapsulated within chitosan-based microcapsules. Firstly, these microcapsules are designed to release the core material upon damage or rupture of the coating, thereby facilitating the repair of the coating. Secondly, upon exposure to air, the microcapsules react with water and carbon dioxide to form carbonic acid, which promotes acid hydrolysis, leading to the rupture of the microcapsules. This process enables the healing agent to fill voids or cracks, restoring the

structural integrity of the coating and extending its service life.

2. Materials and methods

2.1. Materials

Chitosan (CS, 69047436) and triethanolamine were procured as a biological reagent (BR) from Sinopharm Chemical Reagent Co., Ltd. Ethanoic acid (AR) was obtained from Nanjing Chemical Reagent Co., Ltd. Sodium dodecylbenzenesulfonate (SDBS) AR was purchased from Beichen Fangzheng Reagent Factory. Triton X-100 was acquired from Shandong Yousuo Chemical Technology Co., Ltd. Alkylphenol polyoxyethylene ether (OP-10), (O821357) hydrophilic, hydroxyl value 87 ± 10 , Tween 20, and sodium tripolyphosphate (STPP) were purchased from Macklin Biochemical Co., Ltd. (Shanghai, China). Wood wax oil (wwo) was prepared in the laboratory was used as oil phase, raw materials are as follows: thistle oil from Panjin Huacheng Pharmaceutical Co., Ltd., linseed oil, sunflower oil, and soybean oil from Shanghai McLean Biochemical Technology Co., Ltd., carnauba wax (Shandong Yousuo Chemical Technology Co., Ltd.). Naphtha from Shandong ChenYu Chemical Co., Ltd., hand feeling powder SGF-6RM from Heyan Yuese Plastic Pigment Additive Co., Ltd., (Shenzhen China), liquid rosin from Letong Musical Instrument Co., Ltd., isooctanoic acid was purchased from McLean Biochemical Technology Co., Ltd. (Shanghai, China). UV topcoat, composed of epoxy acrylic resin, polyester acrylic resin, TPGDA, TMPTA, photoinitiator, defoaming agent, and leveling agent, was provided by Jiangsu Haitian Technology Co., Ltd. *Escherichia coli* (*E. coli*) and *Staphylococcus aureus* (*S. aureus*) were purchased from BeiJing Baocang Biotechnological Company Limited (Beijing, China).

2.2. Preparation of wood wax oil

In a three-necked flask, a mixture consisting of 54.0 g of linseed oil, 18.0 g of thistle oil, 6.8 g of sunflower seed oil, and 6.8 g of soybean oil was mixed. Under anaerobic conditions, nitrogen gas was introduced through a three-way valve and the temperature was maintained at 110°C under magnetic stirring for 3 h to promote polymerization. Subsequently, 2.7 g of carnauba wax and 0.9 g of beeswax were added and completely dissolved. Upon temperature reduction to 60°C , 18.0 g of rosin, 2.4 g of tactile powder, and 24.0 g of naphtha were introduced into the mixture and stirred for 30 min. Finally, 12.0 g of isooctanoic acid was added and stirring continued for an additional 30 min, an environmentally friendly wood wax oil was obtained.

2.3. Preparation of CS @ wwo microcapsules

The composition of wood wax oil is complex. The majority of the raw materials had HLB values ranging from 7 to 14. For the O/W microcapsules, emulsifiers with HLB values greater than 10 were utilized, indicating their hydrophilic nature. Therefore, SDBS (HLB value

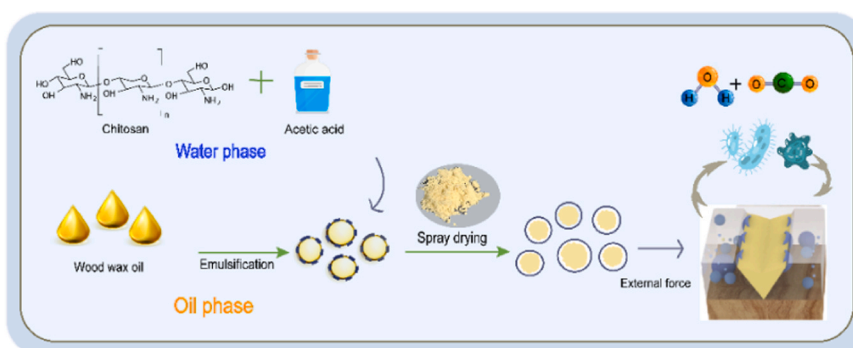


Fig. 1. Schematic diagram of microcapsule preparation.

Table 1

Preparation of microcapsules using different drying methods.

Name	Oil-water ratio	Drying method
S ₁	1:1	Spray drying
F ₁	1:1	Freeze drying
S ₂	2:1	Spray drying
F ₂	2:1	Freeze drying

10.638), OP-10 (HLB value 14.5), Triton X-100 and Tween 20 (mixture HLB value 15) were selected as emulsifier. The dosage of emulsifier is 3.0 %, 5.0 % and 10.0 % respectively. Among them, the compound emulsifier of Triton X-100 and Tween 20 was calculated according to formula (1). The HLB value of Triton X-100 is 14.5, Q_X is the proportion of X-100 in the mixed emulsifier, HLB value of Tween 20 is 16.7, Q_T is the proportion of Tween 20 in the mixed emulsifier.

$$HLB(15) = 14.5Q_X + 16.7Q_T \quad (1)$$

A five factor three-level orthogonal experiment was conducted using oil-water ratio, core to wall ratio, emulsifier type, emulsifier content, and crosslinking agent concentration. The plan table was shown in Table S1, and the specific L27 (3^5) orthogonal experiment table was shown in Table S2.

Taking orthogonal experiment 1 as an example, 1.0 g of aqueous chitosan, 1.0 g of acetic acid, 98.0 mL of deionized water were prepared and stirred at 50 °C and 600 rpm for 1 h to obtain an aqueous phase. A 0.05 g of SDBS and 99.0 mL of deionized water were mixed to prepare an emulsifier, 1.0 g of wood wax oil and emulsifier were emulsified in ultrasonic emulsifier for 10 min, then stirred with magnetic force at 45 °C and 600 rpm for 30 min to obtain oil phase. The core material was slowly added to the wall material, mixed and emulsified with ultrasonic emulsifier for 10 min, the pH was adjusted to 7 with triethanolamine, 18.0 mg/mL STPP solution was added slowly at low temperature, the temperature was raised to 50 °C slowly. The mixed solution continued to be stirred at 1000 rpm for 3 h to form an emulsion. And then it was placed at room temperature for 10 h before freeze drying. The schematic diagram of microcapsule preparation was shown in Fig. 1

The single factor optimization test table was shown in Table 1. Microcapsules were prepared using O/W ratios of 1:1 and 2:1, and then dried using two different methods, freeze drying and spray drying, to obtain the final microcapsules. The spray drying parameters were as follows: an inlet temperature of 110 °C, a feed rate of 100 mL/h, and a spray pressure of 2.0 bar. At the end of the process, pale yellow microcapsules were collected from the cyclone separator assembly. The encapsulation efficiency and yield of the microcapsules were compared to determine the optimal preparation parameters.

2.4. Preparation of UV coatings

A wire rod with a thickness of 30 μm was used, and 2.0, 5.0, 8.0, and 10.0 % chitosan wood wax oil microcapsules were mixed into UV topcoat and applied to the walnut. Each topcoat was cured under a UV lamp for 5 min, and then apply this process 2 times to form a self-healing microcapsule coating.

2.5. Microcapsule encapsulation efficiency and yield

The coating efficiency of microcapsules was measured using solvent extraction method. An amount of 0.5 g of microcapsules was weighed as M_1 . Acetone, in a volume three times that of the microcapsules, was added after grinding and crushing. The mixture was sealed for 72 h, then rinsed, filtered, and dried with ethanol and deionized water. The mass obtained was recorded as M_2 . The encapsulation efficiency of microcapsules is calculated according to formula (2).

$$R\% = \frac{M_1 - M_2}{M_1} \times 100 \quad (2)$$

The actual output of microcapsules is Q_1 , and the total consumption of core material and wall material is Q_2 . The yield of microcapsules is calculated according to formula (3).

$$Y\% = \frac{Q_1}{Q_2} \times 100 \quad (3)$$

2.6. Micromorphology and infrared spectrum

The microscopic morphology of the microcapsules was analyzed by a Quanta-200 scanning electron microscope (SEM). The composition of the microcapsules was tested by a VERTEX 80 V infrared spectrometer (Bruker AG, Karlsruhe, Germany).

2.7. Thermal stability and particle size distribution of microcapsules

Thermogravimetric analysis (TGA) measurements were performed on a TG 209 from TA Instruments to study the thermal stability of the samples. In the heating range of 28 °C to 700 °C, the heating rate is 10 °C/min and the flow rate is 20 mL/min. The particle size distribution of microcapsules was measured using a Malvern laser particle size analyzer.

2.8. Release test

Firstly, in accordance with the environmental conditions of wooden coatings (air), deionized water solutions with pH values of 5.4, 7, and 9 were employed as release mediums. The 0.25, 0.5, 0.75, 1.0, and 1.25 g of wood wax oil were respectively measured into 10 mm diameter colorimetric dishes (capacity 3.5 mL), different pH release mediums were diluted to a final volume of 3.5 mL, resulted in wood wax oil-water solutions with mass concentrations of 0.07 g/mL, 0.14 g/mL, 0.21 g/mL, 0.28 g/mL, and 0.35 g/mL, respectively. Subsequent detection was conducted using a UV-3900 spectrophotometer with a scanning wavelength range of 200–400 nm. After identifying the optimal wavelength for solution absorbance, the absorbance of wood wax at various concentrations was measured at this wavelength. A standard curve correlating concentration and absorbance was then established. The release experiment of wood wax oil from chitosan was conducted to evaluate its stimuli-responsive release behavior and further elucidate the controlled release mechanism of the chitosan microcapsules. A dialysis bags (MWCO = 8000–14000) were utilized to more accurately measure wood wax oil concentration (Cao et al., 2021). The release medium, containing 1.6 g of microcapsules dispersed in 40 mL of solution, was placed into a dialysis bag. Under continuous stirring at a speed of 100 rpm, the dialysis bag was then transferred to another container with 200 mL of the same medium. Subsequently, the ultraviolet absorption of released wood wax oil in the release medium was measured at 296 nm and 293 nm wavelengths using a UV-Vis spectrophotometer (UV-3900 Shimadzu). A 5 mL of dialysate was removed from the release system and immediately replenished with 5 mL of fresh associated release medium. The release percentage is calculated according to formula (4).

$$R_n = \frac{C_n * V + \sum_{i=1}^{n-1} C_i V_1}{m_0} \times 100\% \quad (4)$$

Where R_n is the release percentage of wood wax oil, C_n is the concentration of corrosion inhibitor at the nth sampling, g/mL, V is the volume of release medium, 200 mL, V_1 is the sample volume, 5 mL, m_0 is the mass of wood wax oil encapsulated in the added microcapsules, g.

2.9. Preparation of self-healing coating

Microcapsules at concentrations of 0 %, 2.0 %, 5.0 %, 8.0 %, and

10.0 % were incorporated into UV coatings and cured under a UV lamp. The cured self-healing coatings were then polished with 400-grit sandpaper to simulate everyday damage. The repair effects were visually assessed after 7 d.

2.10. Coating antibacterial test

According to GB/T 21866–2008 “Test method and effect for antibacterial capability of paints film”, agar was mixed with pure water in a certain proportion and placed in a 121 °C oil bath for 30 min. Subsequently, the agar nutrient solution was poured into a culture dish and allowed to solidify. Inoculation loops were used to inoculate *E. coli* and *S. aureus* into petri dishes respectively, which were then cultured for 20 h in a constant temperature and humidity incubator set to 37 °C and 98 % humidity. The broth was mixed with pure water in a certain proportion and placed in an oil bath at 121 °C for 30 min. The inoculation loop was utilized to scrape 1–2 loops of cultured *E. coli* and *S. aureus* into the nutrient broth, and stirred evenly. According to GB/T 4789.2–2022 “the determination of total bacterial colonies in Food Microbiology Inspection”, 10 mL and three 9 mL broth culture solutions were drawn separately for use. One mL of the evenly stirred bacterial broth was transferred into 10 mL of broth dilution. Subsequently, 1 mL of this diluent was sequentially transferred into the next 9 mL of broth dilution, resulting in a final bacterial suspension with a 1000-fold dilution. A 0.5 mL of bacterial suspension was applied to the prepared paint film sample, and the polyethylene film was laid flat on the sample plate to make it evenly contact with the bacterial suspension paint film. The paint film samples were placed in a Petri dish and incubated in a constant temperature and humidity incubator set to 37 °C and 98.0 % humidity for 24 h.

NaCl was utilized to prepare 0.85 % eluent, and it was sterilized in an oil bath at 121 °C for 15 min before use. Two sets of parallel tests were performed on each sample. The samples cultured for 24 h were taken out, 20 mL of eluent was added to each sample, and the sample paint film and covering film were washed repeatedly. After the eluate was stirred evenly, 0.5 mL was inoculated into a flat nutrient agar medium and cultured for 48 h in a constant temperature and humidity box set to 37 °C and 98 % humidity.

The flat nutrient agar medium that had been cultured for 48 h was removed and placed into a colony counter. A precision spot camera was used to take pictures and count the colonies. The average number from the two sets of parallel experiments was recorded as the number of colonies in the sample. The measured number of colonies was multiplied by 1000 to obtain the actual number of viable bacteria recovered after each sample was cultured for 48 h. The antibacterial rate of the paint film was calculated as shown in formula (5). In the formula, R represents the antibacterial rate, B represents the average number of colonies recovered after 48 h in the paint film without added microcapsules, and C represents the average number of colonies recovered after 48 h in the paint film adding microcapsules, the unit is CFU/piece.

$$R = (B - C) / B \times 100\% \quad (5)$$

To determine the minimum inhibitory concentration (MIC) of the microcapsules, a 0.85 % saline solution was prepared and aliquoted into one 10 mL portion and two 9 mL portions. *E. coli* and *S. aureus* were added to the 10 mL saline solution. Then, 1 mL of this solution was transferred to the first 9 mL and second 9 mL saline solution, achieving a 1000-fold dilution. Subsequently, 1 mL of this diluted solution was transferred to 9 mL of broth nutrient solution in a shake tube. Different concentrations of microcapsules (0, 2.0 %, 5.0 %, 8.0 %, and 10.0 %) were added to the tubes, which were then mixed thoroughly. The tubes were incubated at 37 °C for 24 h, after which the turbidity of the broth was observed.

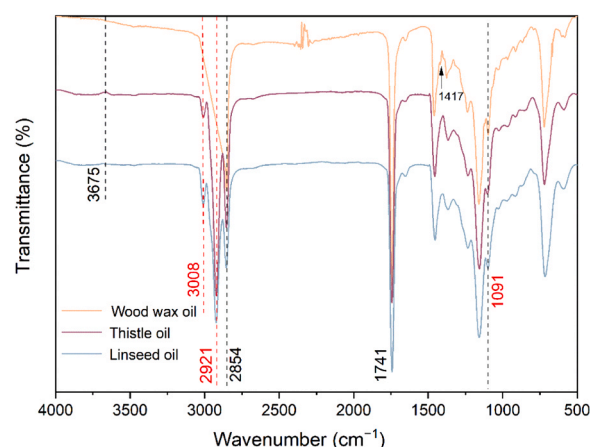


Fig. 2. The infrared spectrum of wood wax oil synthesis.

2.11. Coating adhesion

The adhesion between the coating and the wood substrate was measured using a BEVS 2201 pull-off tester in accordance with the ASTM D4541–02 standard. The surfaces of both the substrate coating and the tensile fixture were polished with 1000-grit sandpaper, and ethanol was used to remove any oil and dust. AB adhesive was mixed thoroughly and applied to the base of the tensile fixture. Each test group consisted of three parallel samples, with one test conducted per group, and the average value was recorded. The pull-off speed was set at 0.8 MPa/s, with a holding force of 10 MPa maintained for 10 s.

3. Results and discussion

3.1. Synthesis of core wood wax oil

The infrared spectrum of wood wax oil synthesis was shown in Fig. 2, after subjecting oil-wax raw materials, primarily consisting of linseed oil and thistle oil, to a high-temperature pre-polymerization process at 110 °C, pronounced changes in the vibrational spectra of specific functional groups were observed. Evidently, the C–H stretching vibrations on the C=C bonds at 3008 cm^{−1} gradually diminished with the high-temperature polymerization of linseed oil and thistle oil. Simultaneously, the O–H stretching vibrations at 2921 cm^{−1} also vanished. Furthermore, a decreasing trend in the O–H stretching vibrations at 3675 cm^{−1} was noted, likely attributed to the hydrolysis reaction of ester bonds in linseed oil. Simultaneously, the C–H of α-linolenic acid, represented by the emergence of the C=C bond at 1417 cm^{−1}, and the –CH functional group at 590 cm^{−1} displayed weakened vibrational peaks following the oil polymerization process (Rosu et al., 2018). The peak at 1091 cm^{−1} corresponds to the C–O bond enhancement in wood wax oil. This phenomenon indicated a reduction in the active hydrogen concentration of the resulting wood wax, signifying that a polymerization reaction occurred within the plant oil-wax system. (Peng et al., 2020).

3.2. Orthogonal test analysis of microcapsule yield and encapsulation efficiency

The encapsulation efficiency and yield results of L27 (3⁵) chitosan microcapsules were shown in Table 2. The mean impact table was calculated through Minitab software. The results showed that the greatest impact on the microcapsule encapsulation efficiency was the emulsifier content. The second was the oil-water ratio. The optimal preparation parameters of chitosan-coated wood wax oil microcapsules were determined based on the mean response table in Table 3. The preferable manufacturing conditions entail an OWR of 2:1, a core-to-

Table 2

Results of orthogonal experimental encapsulation rate and yield.

Factor	Oil to water ratio	Core to wall ratio	Emulsifier	STPP (%)	Emulsifier content (%)	Encapsulation efficiency (%)	Yield (%)
1	1 : 1	1 : 1	SDBS	0.18	5.0	46.4	93.1
2	1 : 1	1 : 1	SDBS	0.18	8.0	53.5	64.5
3	1 : 1	1 : 1	SDBS	0.18	10.0	68.0	79.3
4	1 : 1	2 : 1	OP-10	0.36	5.0	51.0	72.5
5	1 : 1	2 : 1	OP-10	0.36	8.0	64.2	76.0
6	1 : 1	2 : 1	OP-10	0.36	10.0	62.8	91.9
7	1 : 1	3 : 1	X100-T20	0.50	5.0	65.4	64.7
8	1 : 1	3 : 1	X100-T20	0.50	8.0	49.6	57.9
9	1 : 1	3 : 1	X100-T20	0.50	10.0	58.4	64.9
10	1.5 : 1	1 : 1	OP-10	0.50	5.0	52.4	78.9
11	1.5 : 1	1 : 1	OP-10	0.50	8.0	44.6	94.3
12	1.5 : 1	1 : 1	OP-10	0.50	10.0	25.2	108.9
13	1.5 : 1	2 : 1	X100-T20	0.18	5.0	48.4	41.7
14	1.5 : 1	2 : 1	X100-T20	0.18	8.0	49.2	43.6
15	1.5 : 1	2 : 1	X100-T20	0.18	10.0	50.2	37.9
16	1.5 : 1	3 : 1	SDBS	0.36	5.0	36.8	56.6
17	1.5 : 1	3 : 1	SDBS	0.36	8.0	82.6	50.0
18	1.5 : 1	3 : 1	SDBS	0.36	10.0	52.0	56.6
19	2 : 1	1 : 1	X100-T20	0.36	5.0	26.4	59.0
20	2 : 1	1 : 1	X100-T20	0.36	8.0	67.5	60.2
21	2 : 1	1 : 1	X100-T20	0.36	10.0	91.4	90.1
22	2 : 1	2 : 1	SDBS	0.50	5.0	45.7	71.6
23	2 : 1	2 : 1	SDBS	0.50	8.0	14.5	38.0
24	2 : 1	2 : 1	SDBS	0.50	10.0	78.5	40.2
25	2 : 1	3 : 1	OP-10	0.18	5.0	61.4	30.3
26	2 : 1	3 : 1	OP-10	0.18	8.0	85.5	27.6
27	2 : 1	3 : 1	OP-10	0.18	10.0	96.3	25.2

Table 3

Mean response table.

Factor	OWR	Core to wall ratio	Emulsifier	STPP (%)	Emulsifier content (%)
1	57.70	52.82	60.36	62.09	48.20
2	49.04	51.61	53.11	59.41	56.80
3	63.01	65.32	56.28	48.25	64.75
Delta	13.96	13.71	7.26	13.84	16.55
Rank	2	4	5	3	1

wall ratio of 3:1, the utilization of OP-10 as the emulsifier at a concentration of 10.0 %, and a STPP concentration of 0.18 g/mL. The function of STPP as a cross-linking agent lies in its ability to interact with chitosan, thereby forming a compact shell structure, which serves to safeguard the core material and prolong its release kinetics.

3.3. Orthogonal test micromorphology analysis

The morphology of the 27 microcapsules prepared was shown in Fig. 3. There are formed microcapsules in the scanning electron microscopy with chitosan microcapsules possessing diameters about 5 μm , the shape was amorphous, and there was a little spherical structure. The morphology appears amorphous with occasional spherical structures, although a majority of the microcapsules were agglomerated. This phenomenon was attributed to the incomplete homogenization of the oil and water phases, where the differing shear forces induced by simple magnetic stirring resulted in inadequate dispersion. The reticular structure formed during the cross-linking of STPP with CS leads to continued aggregation of already formed microcapsules, thus diminishing dispersion efficacy. Wood wax oil, being sparingly soluble in water, primarily nucleated through micellar formation. When the OWR exceeded 1, the presence of 10.0 % emulsifier along with water molecules facilitated thorough emulsification of the wood wax oil. However, incomplete emulsification during the blending of core and shell materials resulted in reduced encapsulation efficiency. Additionally, freeze-dried microcapsules were prone to volume shrinkage and increased hardness.

3.4. Microscopic analysis of microcapsules with different OWR and drying method

The SEM images of different OWRs and different drying method were shown in Fig. 4 and Table 4. Fig. 4(a₁) showed the S₁ OWR of 1:1 microcapsule exhibited predominantly intact and regularly spherical structures, albeit with some instances of adhesion. In Fig. 4(a₂), an enlarged view of microcapsule morphology revealed a particle size of approximately 5 μm , with surface wrinkling and adhesion. This phenomenon may have arisen from the rapid temperature elevation during spray drying, which caused the chitosan shell material to undergo shrinkage. The particle size distribution for an OWR of 1:1 was depicted in Fig. 4(a₃), with most microcapsules distributed around 7 μm , accounting for 34.0 %. The spray-dried microcapsules with an S₂ OWR of 2:1 was depicted in Fig. 4(b₁), which exhibited a complete spherical structure and good dispersion. However, as depicted in Fig. 4(b₂), surface wrinkling was still evident. The adhesion of microcapsules at an OWR of 1:1 appears greater compared to the ratio of 2:1. This disparity was attributed to inadequate water content in the oil phase, which resulted in the incomplete dispersion of oil droplets during emulsification. The particle size distribution for microcapsules with an OWR of 2:1 was illustrated in Fig. 4(b₃). Microcapsules with sizes ranging from 3 to 4 μm accounted for 28 %, and those from 4 to 5 μm accounted for 22 %, resulting in 50 % of the microcapsules falling within the 3–5 μm range. Other sizes were relatively infrequent. This indicated that microcapsules with an OWR of 2:1 exhibit smaller particle sizes and a more concentrated distribution. Fig. 4(c) presented the freeze-dried microcapsules with an OWR of 1:1. The number of complete spherical microcapsules was limited, with the majority exhibiting an amorphous structure. Nevertheless, they retained their encapsulation efficiency. The microcapsules with an OWR of 2:1, as depicted in Fig. 4(d), were subjected to freeze drying. Although this ratio represented an improvement over the 1:1 OWR, the resulting morphology remained suboptimal, appearing flaky and amorphous. During the spray drying process, the emulsion was rapidly atomized into small droplets. The oil-phase core material was encapsulated by the water-phase wall material, and the water quickly evaporated at the high air outlet temperature. This process formed a protective film from the water phase, effectively encapsulating the oil

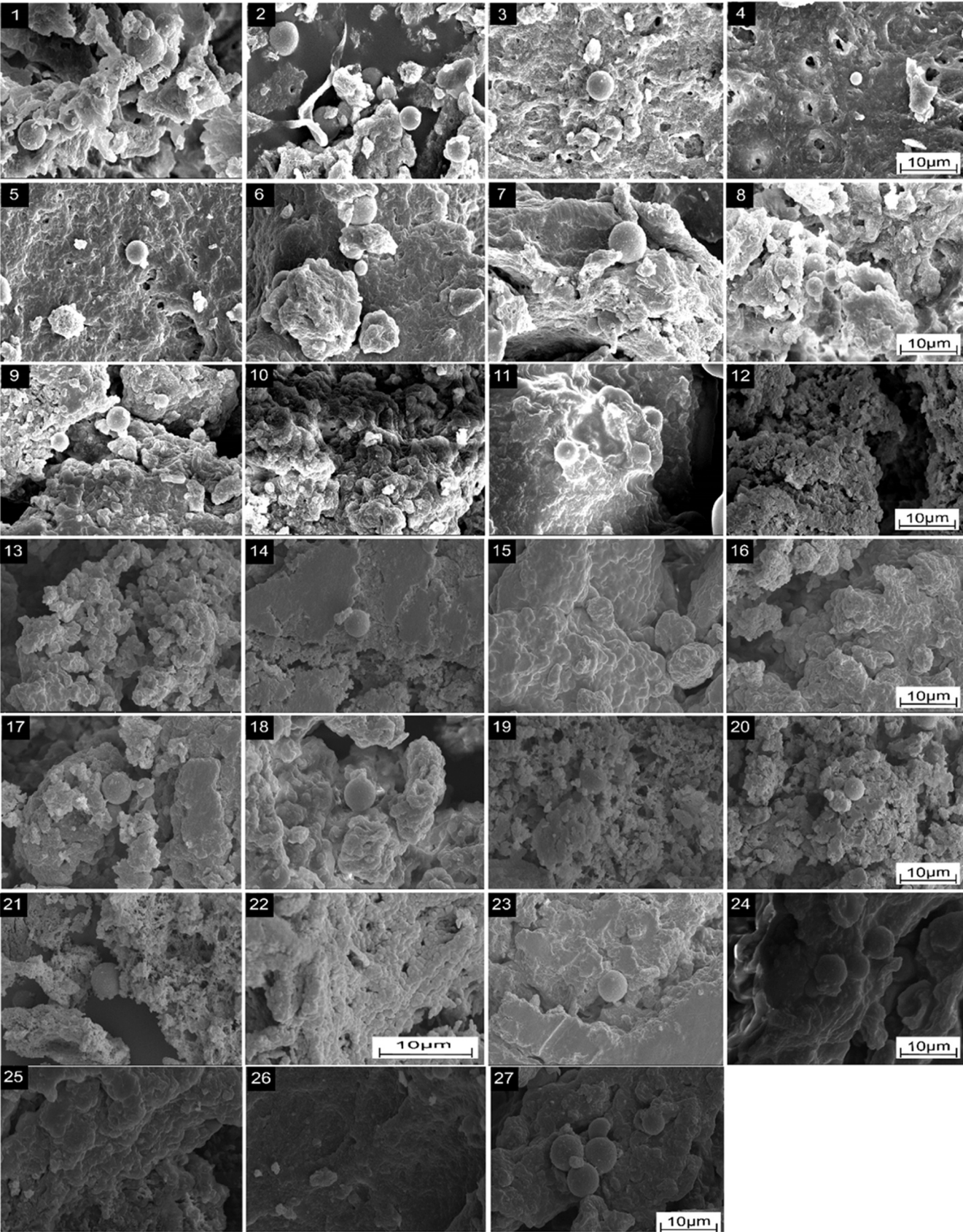


Fig. 3. Orthogonal experimental scanning electron microscopy image.

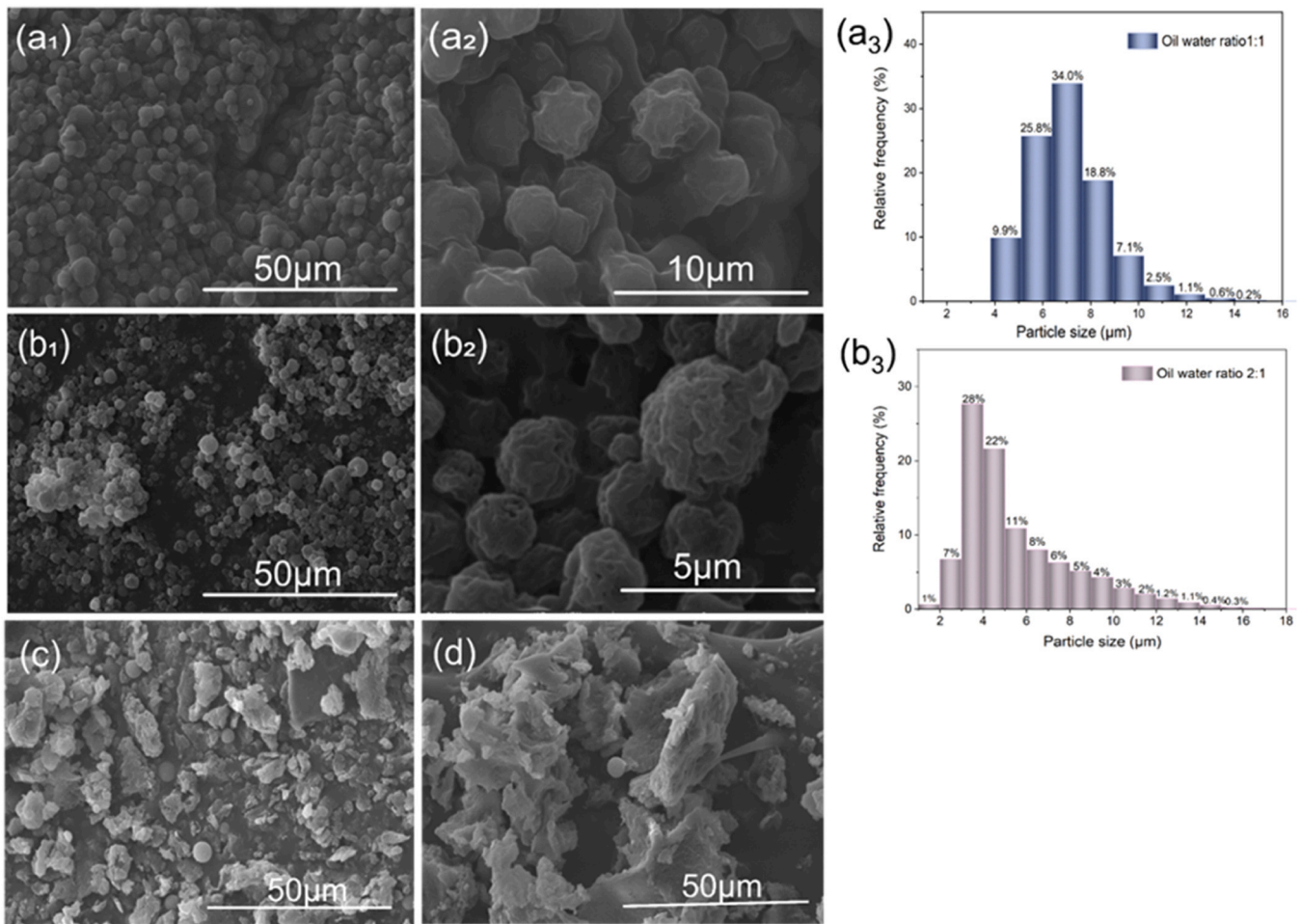


Fig. 4. (a₁) S₁ microcapsule, (b₁) S₂ microcapsule, (a₃) OWR 1:1 particle size distribution, (b₃) OWR 2:1 particle size distribution. (c) F₁ microcapsule, (d) F₂ microcapsule.

Table 4
Encapsulation efficiency of microcapsules under different drying methods.

Name	OWR	Drying method	Encapsulation efficiency (%)	Yield (%)
S ₁	1:1	Spraying drying	67.5±1.9	63.4±1.1
F ₁	1:1	Freeze drying	70.5±2.3	72.6±1.3
S ₂	2:1	Spraying drying	73.7±2.5	68.9±2.3
F ₂	2:1	Freeze drying	96.2±2.6	25.2±1.2

within (Eun et al., 2020). A higher entrapment rate indicated a greater degree of protection for the oil phase and enhanced the quality of the microcapsules. Ice crystals formed when the emulsion was pre-frozen, disrupting the 'aqueous liquid film' that had formed on the outer layer of the core material after homogenization. This exposure of the core material resulted in a reduced embedding rate (Tonon et al., 2011). It was concluded that spray drying had lower production costs, shorter drying times, and a larger specific surface area. Additionally, the microcapsules produced through this method exhibited a complete spherical morphology and uniform particle size (Wang et al., 2008). The encapsulation efficiency of microcapsules in different drying methods were shown in Table 4. F₂ microcapsules showed the highest encapsulation efficiency of 96.2 %, but the lowest yield. Considering the S₂ OWR of 2:1, the spray-dried microcapsules exhibited better morphology and encapsulation efficiency.

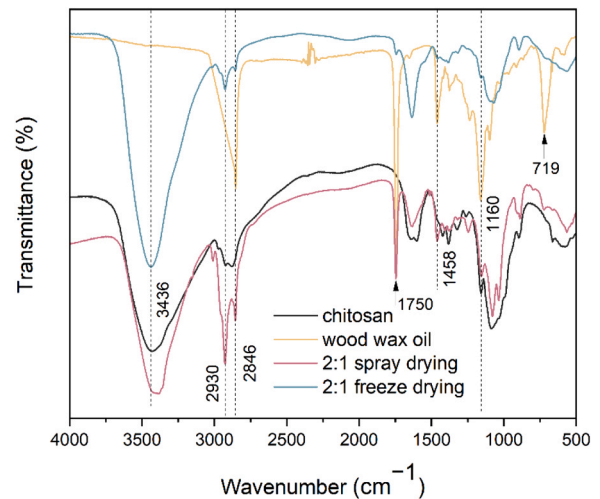


Fig. 5. Infrared spectroscopy of CS@wwo microcapsules.

3.5. Infrared spectroscopic analysis of microcapsules

The infrared spectra of chitosan, wood wax oil, and microcapsules with different drying methods were shown in Fig. 5. 3436 cm⁻¹ is the OH stretching vibration absorption peak in chitosan, the stretching vibration of methyl groups in wood wax oil was observed at 1458 cm⁻¹.

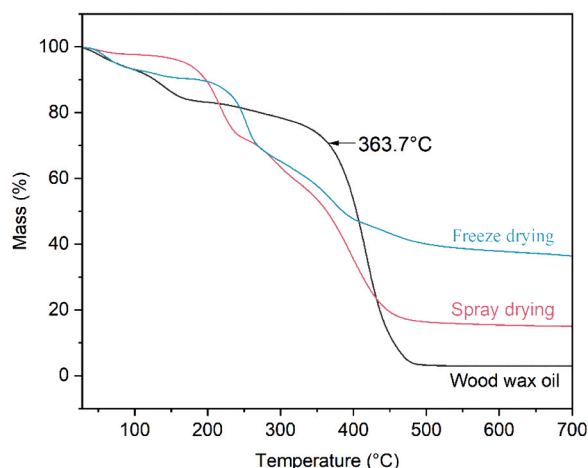


Fig. 6. Thermogravimetric analysis of chitosan wood wax oil microcapsules with different drying methods.

The characteristic peak was weakened, indicating that the wood wax oil had been successfully coated with chitosan. Additionally, the C=C double bond vibration at 1160 cm^{-1} decreased or even disappeared in the microcapsules, further indicating the successful encapsulation of the wood wax oil. The C=O-OR ester group in wood wax oil was observed at 1750 cm^{-1} , and CH_2 was observed at 2846 cm^{-1} . Both characteristic peaks were weakened and appeared in the infrared spectra of the microcapsules. Additionally, the characteristic peak of the unsaturated bond bending vibration, =C-H, at 719 cm^{-1} disappeared in the

microcapsules. These observations further confirmed the successful encapsulation of wood wax oil by chitosan.

3.6. Thermal stability of microcapsules

The thermogravimetric analysis of CS@wwo microcapsules with different drying methods was depicted in Fig. 6. The mass loss of the microcapsules dried by 2:1 spray at 187°C began in the first stage, during which the chitosan shell started to decompose. The quality loss of wood wax oil was relatively small at the first 200°C . At 363.7°C , wood wax oil begins to decompose, and there was still 14.94 % residual quality at 700°C . In contrast, microcapsules subjected to freeze drying commenced mass loss at 46.1°C , suggesting an earlier onset of decomposition due to the less dense structure of the chitosan wall material. The spray drying method facilitated effective protection of the wood wax oil core by chitosan, thereby ensuring the compactness and stability of the microcapsule structure. (Lai et al., 2021).

3.7. Release behavior analysis

The release amount of wood wax oil was determined by ultraviolet spectrophotometry, and the release behavior of the microcapsule repair agent was analyzed by the concentration change of wood wax oil released at different times. The characteristic ultraviolet absorption wavelength of wood wax oil in an aqueous solution with pH 5.4 was 294 nm , while in aqueous solutions with pH 7 and 9, the characteristic wavelength was 293 nm , as shown in Fig. 7(a). Therefore, 294 nm and 293 nm were selected as the ultraviolet absorption wavelengths for wood wax oil in the subsequent release media with pH values of 5.4, 7,

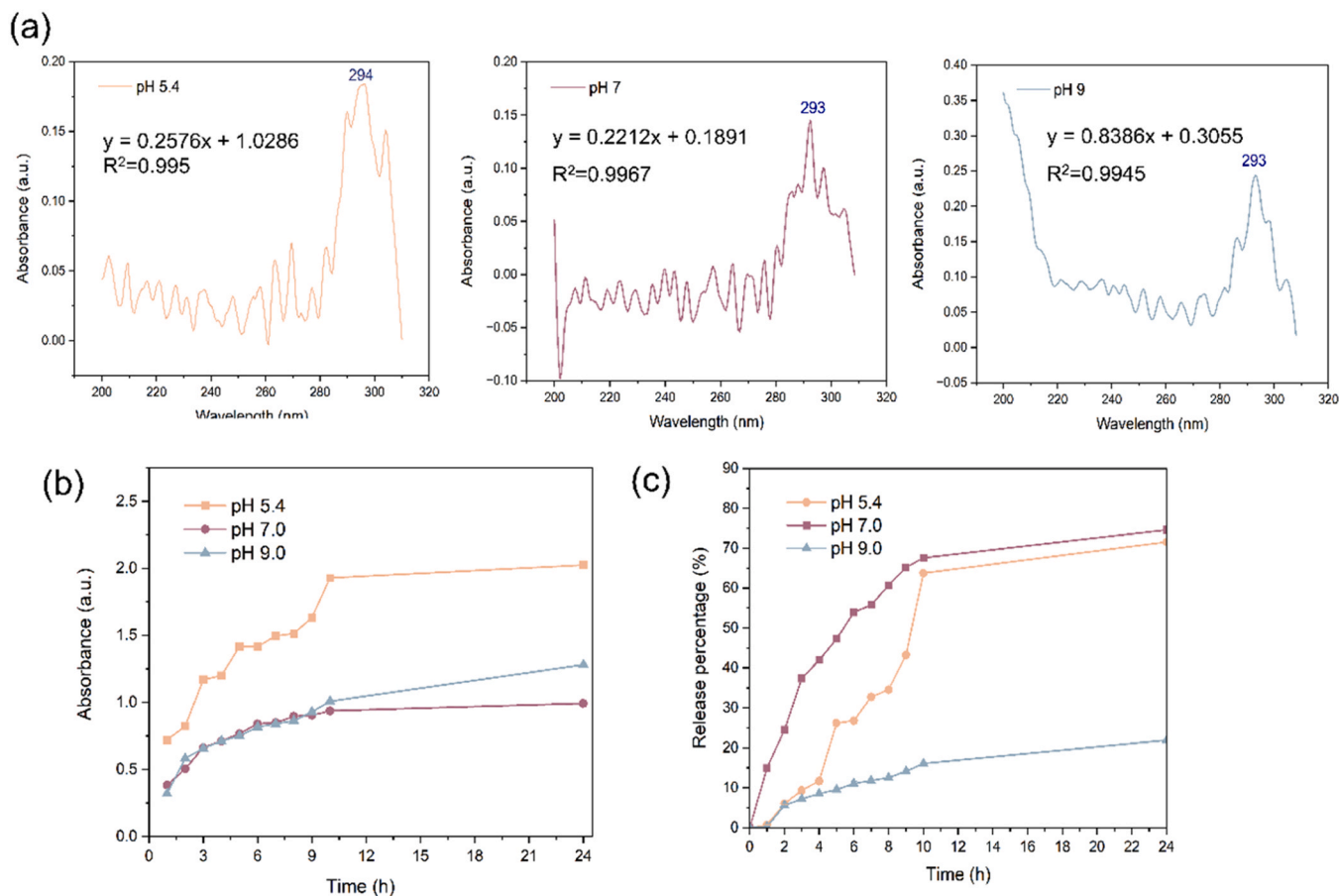


Fig. 7. (a) UV absorption curves of wood wax oil in aqueous solutions of different pH values, (b) Absorbance of microcapsules in different release media (c) Release percentage of microcapsules in different release media.

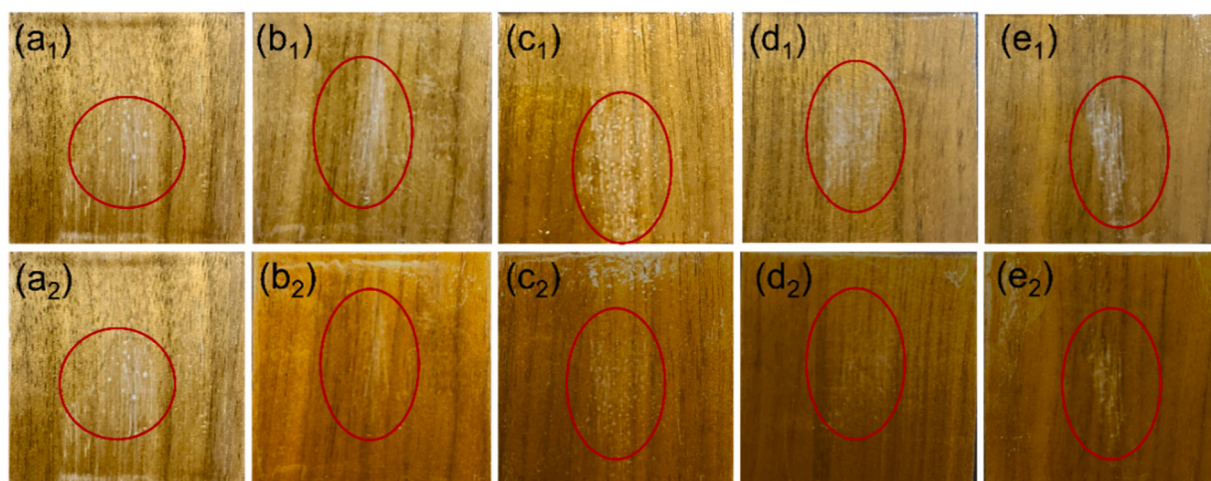


Fig. 8. Diagram before and after repair of microcapsule coating. The a–e microcapsule contents are 0, 2.0 %, 5.0 %, 8.0 % and 10.0 % respectively. The number 1 represents the state prior to repair, while number 2 illustrates the condition subsequent to repair.

and 9, respectively. The standard sample curves of wood wax oil in different media were measured using standard solutions of wood wax oil at different concentrations. The R^2 values were greater than 0.99, indicating that the standard curves could be used for subsequent concentration calculations. The absorbance and release percentages of the microcapsules in different release media were presented in Fig. 7(b) and (c). As depicted in Fig. 7(c), the absorbance of wood wax oil was higher at pH 5.4, illustrated that at pH 5.4, the highest release percentage of wood wax oil reached 70.6 %. At pH 7.0, the release percentage was the highest, reaching 74.6 %. The release amount of the microcapsules at pH 5.4 and 7.0 exceeded 70.0 %, whereas at pH 9.0, the release amount was only 22.2 %. This indicated that CS @ wwo microcapsules exhibited characteristics of water-sensitive and acid-selective responses. Wood wax oil was continuously released for 24 h in environments of pH 5.4 and 7.0, with the release amount surpassing 70 %. This suggested that CS @ wwo microcapsules could be continuously released in these environments to achieve a rapid and sustained repair effect.

3.8. Microcapsule self-healing coating

Self-healing paint films with different microcapsule contents were shown in Fig. 8. After simulated scratches with 400-grit sandpaper, the surface of the paint film turned white. After 7 d, it was observed that the surface of the paint film without the addition of microcapsules still maintained its original morphology. The whitening of the surface of 2.0–8.0 % of the microcapsules was effectively repaired, while the scratches on the surface of the 10.0 % paint film were more serious. There is still an intuitive improvement effect.

3.9. Antibacterial properties of coating

Antibacterial pictures, antibacterial rates and IC_{50} of antibacterial microcapsules wood coating were displayed in Fig. 9. It was observed that the number of colonies without microcapsules was significantly greater than that with microcapsules, indicating the antibacterial properties of the microcapsules. The colony diagrams of *E. coli* and *S. aureus* were presented in Fig. 9(a), where the growth of the colonies could be clearly observed. Fig. 9(b) indicated that CS @ wwo microcapsules exhibited better antibacterial properties against *E. coli* than *S. aureus*. The antibacterial efficacy of the coating increased with the higher addition of microcapsules, achieving a maximum antibacterial rate of 75.82 % against *E. coli* and 42.96 % against *S. aureus*. The antibacterial mechanism of wood wax oil against *E. coli* was attributed to the inhibitory effect of silymarin present in thistle oil. (Fekri Kohan et al.,

2024) Additionally, chitosan inherently disrupted the structural integrity of both *E. coli* and *S. aureus*, resulting in the leakage of enzymes and nucleotides from various cellular locations. (Chung and Chen, 2008; Zhou and Xu, 2024) The IC_{50} of wood coatings against *E. coli* was shown in Fig. 9(c), when the inhibitory rate reached 50.0 %, the required concentration of microcapsules was 5.677 %, corresponding to an IC_{50} value of 5.677. The IC_{50} of wood coatings against *S. aureus* was shown in Fig. 9(d), at an inhibitory rate of 50.0 %, the necessary concentration of microcapsules was 15.45 %, corresponding to an IC_{50} value of 15.45. Fig. 9(e) illustrated the MIC of the microcapsules against *E. coli*. The control broth nutrient solution remained clear, whereas the solution without microcapsules became turbid, indicating the growth of *E. coli*. As the concentration of microcapsules increased, the broth nutrient solution gradually cleared, indicating that a 10.0 % microcapsule concentration constituted the MIC. Fig. 9(f) presented the MIC of the microcapsules against *S. aureus*, with the observed turbidity in the broth being consistent with that seen for *E. coli*.

3.10. Coating adhesion

The results of the pull-off tests for various microcapsule contents were presented in Fig. 10. The adhesion initially increased with the microcapsule mass fraction, reaching its peak when the mass fraction was 2.0 %. However, when the microcapsule content exceeds 5.0 %, a significant decrease in adhesion was observed. This decline was attributed to the excessive mass fraction of microcapsules, which increased the solid content of the coating. Additionally, the spherical structure of the microcapsules reduced the contact area between the coating and the walnut substrate, thereby diminishing adhesion.

4. Conclusion

The optimal preparation process for the microcapsules involved using chitosan at a concentration of 1.0 %, an OWR of 2:1, and a core-to-wall ratio of 3:1. The emulsifier OP-10 demonstrated the best emulsification effect, with an emulsifier content of 10.0 % and STPP content of 0.18 g/mL at pH 7. The drying method employed was spray drying. These microcapsules exhibited selective responsiveness to water and acid, effectively releasing their contents over 24 h, with a release rate of 74.6 % in neutral water. The microcapsules were incorporated into UV topcoat to prepare walnut multilayer wood coatings, achieving effective scratch repair within 7 d. The antibacterial rates of the 10.0 % microcapsule coatings were 75.82 % against *E. coli* and 42.96 % against *S. aureus*. The IC_{50} of the wood coatings against *E. coli* was 5.667, while

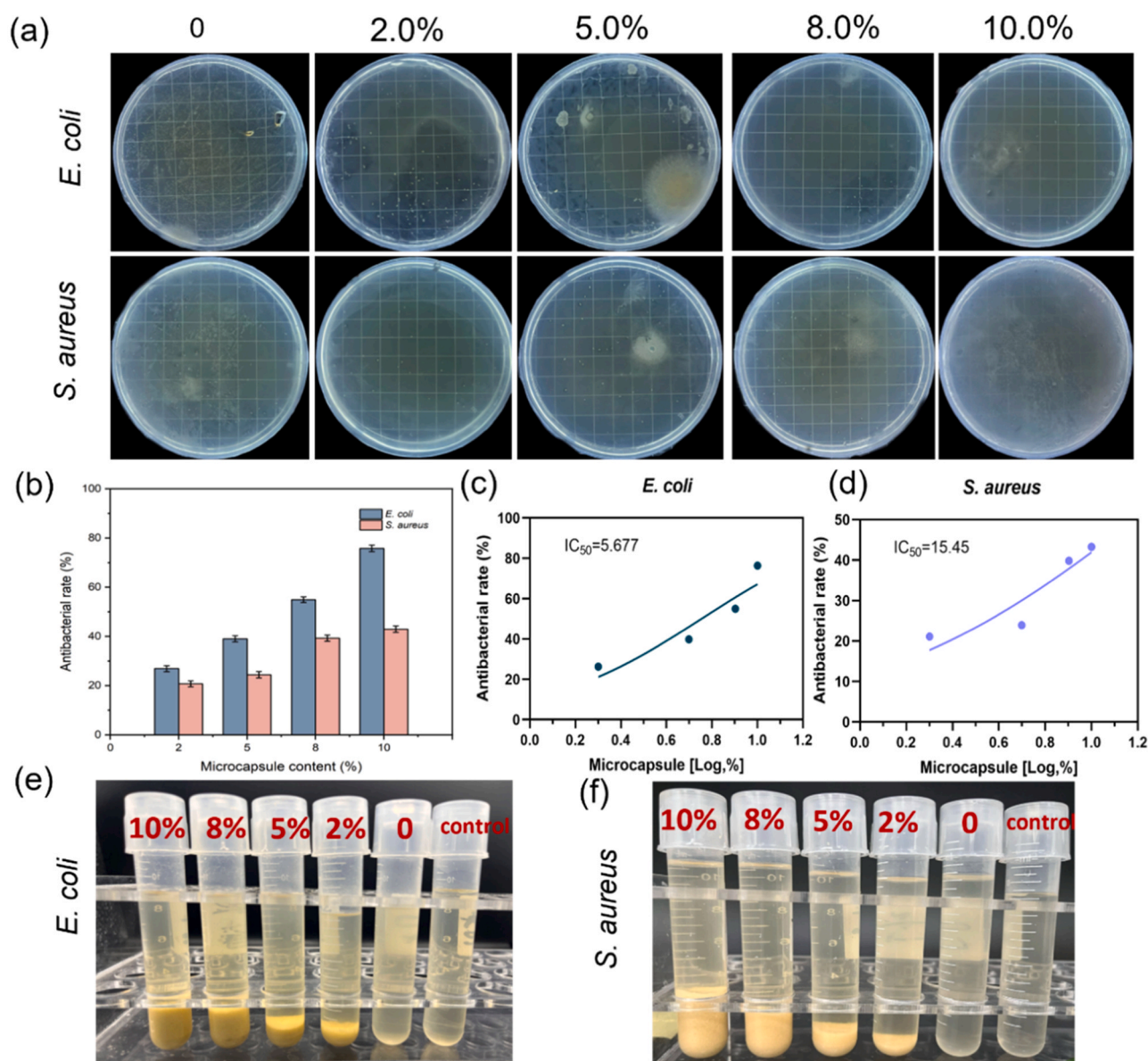


Fig. 9. (a) Antibacterial picture, (b) antibacterial rate, (c) IC_{50} of wood coating against *E. coli*, (d) IC_{50} of wood coating against *S. aureus*, (e) MIC of microcapsule against *E. coli*, (f) MIC of microcapsule against *S. aureus*.

against *S. aureus* it was 15.45. The minimum inhibitory concentration (MIC) of the microcapsules against both *E. coli* and *S. aureus* was 10.0 %. The UV topcoat film containing 2.0 % microcapsules demonstrates superior overall performance. The chitosan wood wax oil microcapsules developed in this study had the potential to lay the foundation for multifunctional, intelligent, and responsive wood coatings.

Funding

This work was funded by the National Key Research and Development Program (nos. 2016YFD0600704, 2018YFD0600304, and 2023YFD2201501) and Graduate Research and Innovation Projects of Jiangsu Province (grant no. KYCX23_1195).

CRediT authorship contribution statement

Zhihui Wu: Writing – review & editing, Supervision, Methodology, Funding acquisition, Conceptualization. **Yijuan Chang:** Writing – original draft, Visualization, Investigation, Formal analysis, Data

curation. **Enwen Liu:** Visualization, Data analysis, Graph Plotting, Writing - original draft.

Declaration of Competing Interest

The author declared that they have no conflicts of interest to this work. We declare that we do not have any commercial or associative interest that represents a conflict of interest in connection with the work submitted.

Data availability

Data will be made available on request.

Appendix A. Supporting information

Supplementary data associated with this article can be found in the online version at [doi:10.1016/j.indcrop.2024.119438](https://doi.org/10.1016/j.indcrop.2024.119438).

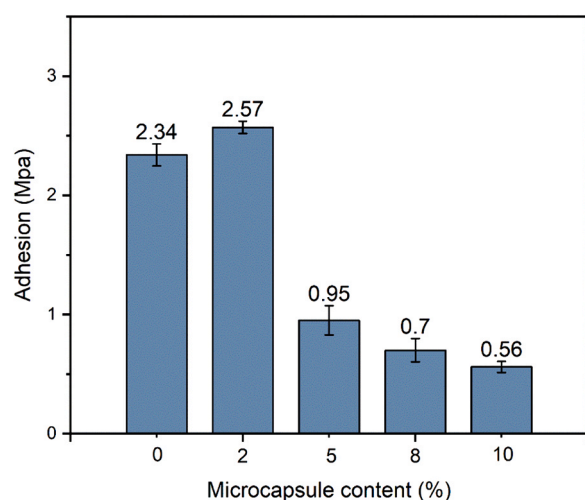


Fig. 10. Coating adhesion of different microcapsule mass fractions.

References

- Abbaspourrad, A., Carroll, N.J., Kim, S.-H., Weitz, D.A., 2013. Polymer microcapsules with programmable active release. *J. Am. Chem. Soc.* 135, 7744–7750.
- Bakry, A.M., Abbas, S., Ali, B., Majeed, H., Abouelwafa, M.Y., Mousa, A., Liang, L., 2016. Microencapsulation of oils: a comprehensive review of benefits, techniques, and applications. *Compr. Rev. Food Sci. Food Saf.* 15, 143–182.
- Budinčić, J.M., Petrović, L., Đekić, L., Fraj, J., Bučko, S., Katona, J., Spasojević, L., 2021. Study of vitamin E microencapsulation and controlled release from chitosan/sodium lauryl ether sulfate microcapsules. *Carbohydr. Polym.* 251, 116988.
- Cao, Y., Yuan, X., Wang, X., Li, W., Yang, H., 2021. Synthesis and controlled release kinetics of pH-sensitive hollow polyaniline microspheres encapsulated with the corrosion inhibitor. *J. Mol. Liq.* 342, 117497.
- Chang, S.-T., Chou, P.-L., 2000. Photodiscoloration inhibition of wood coated with UV-curable acrylic clear coatings and its elucidation. *Polym. Degrad. Stab.* 69, 355–360.
- Chang, Y., Wu, Z., 2024. Synthesized high performance UV-cured wood wax oil using Irgacure 2959 modified thistle oil and linseed oil. *Ind. Crops Prod.* 218, 118952.
- Chung, Y.-C., Chen, C.-Y., 2008. Antibacterial characteristics and activity of acid-soluble chitosan. *Bioresour. Technol.* 99, 2806–2814.
- De Meijer, M., 2001. Review on the durability of exterior wood coatings with reduced VOC-content. *Prog. Org. Coat.* 43, 217–225.
- Deng, J., Huang, N., Yan, X., 2023. Effect of composite addition of antibacterial/ photochromic/self-repairing microcapsules on the performance of coatings for medium-density fiberboard. *Coatings* 13, 1880.
- Ding, T., Yan, X., 2024. Preparation process optimization for melamine resin-covered pomelo peel flavonoid antibacterial microcapsules and their effect on waterborne paint film performance. *Coatings* 14, 654.
- Eun, J.-B., Maruf, A., Das, P.R., Nam, S.-H., 2020. A review of encapsulation of carotenoids using spray drying and freeze drying. *Crit. Rev. Food Sci. Nutr.* 60, 3547–3572.
- Fei, X., Zhao, H., Zhang, B., Cao, L., Yu, M., Zhou, J., Yu, L., 2015. Microencapsulation mechanism and size control of fragrance microcapsules with melamine resin shell. *Colloids Surf. A: Physicochem. Eng. Asp.* 469, 300–306.
- Fekri Kohan, S., Nouhi Kararoudi, A., Bazgosha, M., Adelifar, S., Hafezolzhorani Esfahani, A., Ghaderi Barmi, F., Kouchakinejad, R., Barzegari, E., Shahriarinnour, M., Ranji, N., 2024. Determining the potential targets of silybin by molecular docking and its antibacterial functions on efflux pumps and porins in uropathogenic *E. coli*. *Int. Microbiol.*
- Gouin, S., 2004. Microencapsulation: industrial appraisal of existing technologies and trends. *Trends Food Sci. Technol.* 15, 330–347.
- Janesch, J., Arminger, B., Gindl-Altmutter, W., Hansmann, C., 2020. Superhydrophobic coatings on wood made of plant oil and natural wax. *Prog. Org. Coat.* 148, 105891.
- Koçak, Ö.F., Yılmaz, F., 2022. Use of alpinia officinarum rhizome in textile dyeing and gaining simultaneous antibacterial properties. *J. Nat. Fibers* 19, 1925–1936.
- Kumar, S., Mukherjee, A., Dutta, J., 2020. Chitosan based nanocomposite films and coatings: emerging antimicrobial food packaging alternatives. *Trends Food Sci. Technol.* 97, 196–209.
- Lai, H., Liu, Y., Huang, G., Chen, Y., Song, Y., Ma, Y., Yue, P., 2021. Fabrication and antibacterial evaluation of peppermint oil-loaded composite microcapsules by chitosan-decorated silica nanoparticles stabilized Pickering emulsion templating. *Int. J. Biol. Macromol.* 183, 2314–2325.
- Liu, F., Liu, A., Tao, W., Yang, Y., 2020. Preparation of UV curable organic/inorganic hybrid coatings-a review. *Prog. Org. Coat.* 145, 105685.
- Meng, Q., Zhong, S., Wang, J., Gao, Y., Cui, X., 2023. Advances in chitosan-based microcapsules and their applications. *Carbohydr. Polym.* 300, 120265.
- Mwangi, W.W., Ho, K.-W., Ooi, C.-W., Tey, B.-T., Chan, E.-S., 2016. Facile method for forming ionically cross-linked chitosan microcapsules from Pickering emulsion templates. *Food Hydrocoll.* 55, 26–33.
- Nesterenko, A., Alric, I., Silvestre, F., Durrieu, V., 2014. Comparative study of encapsulation of vitamins with native and modified soy protein. *Food Hydrocoll.* 38, 172–179.
- Peng, Y., Wang, Y., Chen, P., Wang, W., Cao, J., 2020. Enhancing weathering resistance of wood by using bark extractives as natural photostabilizers in polyurethane-acrylate coating. *Prog. Org. Coat.* 145, 105665.
- Rawat, R.S., Chouhan, N., Talwar, M., Diwan, R.K., Tyagi, A.K., 2019. UV coatings for wooden surfaces. *Prog. Org. Coat.* 135, 490–495.
- Rosu, L., Varganici, C.-D., Mustata, F., Rusu, T., Rosu, D., Rosca, I., Tudorachi, N., Teacă, C.-A., 2018. Enhancing the thermal and fungal resistance of wood treated with natural and synthetic derived epoxy resins. *ACS Sustain. Chem. Eng.* 6, 5470–5478.
- Samadzadeh, M., Boura, S.H., Peikari, M., Kasiriha, S.M., Ashrafi, A., 2010. A review on self-healing coatings based on micro/nanocapsules. *Prog. Org. Coat.* 68, 159–164.
- Tonon, R.V., Grosso, C.R.F., Hubinger, M.D., 2011. Influence of emulsion composition and inlet air temperature on the microencapsulation of flaxseed oil by spray drying. *Food Res. Int.* 44, 282–289.
- Wang, T., Li, L., Cao, Y., Wang, Q., Guo, C., 2019. Preparation and flame retardancy of castor oil based UV-cured flame retardant coating containing P/Si/S on wood surface. *Ind. Crops Prod.* 130, 562–570.
- Wang, J.-X., Wang, Z.-H., Chen, J.-F., Yun, J., 2008. Direct encapsulation of water-soluble drug into silica microcapsules for sustained release applications. *Mater. Res. Bull.* 43, 3374–3381.
- Wu, Y., Wu, X., Yang, F., Zhang, H., Feng, X., Zhang, J., 2020. Effect of thermal modification on the nano-mechanical properties of the wood cell wall and waterborne polyacrylic coating. *Forests* 11, 1247.
- Wu, M., Xue, Z., Wang, C., Wang, T., Zou, D., Lu, P., Song, X., 2024. Smart antibacterial nanocellulose packaging film based on pH-stimulate responsive microcapsules synthesized by Pickering emulsion template. *Carbohydr. Polym.* 323, 121409.
- Xia, Y., Yan, X., 2024. Preparation of UV topcoat microcapsules and their effect on the properties of UV topcoat paint film. *Polymers* 16, 1410.
- Yilmaz, F., 2020. Investigation of antibacterial effect of hypericum perforatum l. on woolen fabrics. *AATCC J. Res.* 7, 22–26.
- Yilmaz, F., 2023. Application of achillea millefolium as a natural antibacterial agent in finishing of textile. *Fibers Polym.* 24, 3175–3182.
- Yilmaz, F., Bahtiyari, M.I., 2020. Use of tea and tobacco industrial wastes in dyeing and antibacterial finishing of cotton fabrics. *AATCC J. Res.* 7, 25–31.
- Yousefi, M., Khorshidian, N., Mortazavian, A.M., Khosravi-Darani, K., 2019. Preparation optimization and characterization of chitosan-tripolyphosphate microcapsules for the encapsulation of herbal galactagogue extract. *Int. J. Biol. Macromol.* 140, 920–928.
- Zhang, H., Gan, J., Wu, Y., Wu, Z., 2023. Biomimetic high water adhesion superhydrophobic surface via UV nanoimprint lithography. *Appl. Surf. Sci.* 633, 157610.
- Zhou, J., Xu, W., 2024. A fast method to prepare highly isotropic and optically adjustable transparent wood-based composites based on interface optimization. *Ind. Crops Prod.* 218, 118898.
- Zhu, Y., Li, W., Xia, Y., Hang, J., Yan, X., Li, J., 2024. Effect of blending of shellac, carbonyl iron powder, and carbonyl iron powder/carbon nanotube microcapsules on the properties of coatings. *Coatings* 14, 75.
- Zou, Y., Pan, P., Yan, X., 2023. Comparative analysis of performance of water-based coatings prepared by two kinds of anti-bacterial microcapsules and nano-silver solution on the surface of andoung wood. *Coatings* 13, 1518.
- Zou, Y., Pan, P., Zhang, N., Yan, X., 2024. Effect of nano-silver solution microcapsules mixed with rosin-modified shellac microcapsules on the performance of water-based coating on Andoung wood (*Monopetalanthus* spp.). *Coatings* 14, 286.